Experimental Investigation of Tensile Properties of Stainless Steel Mesh as a Cost-Effective Strengthening Material

Harsono, Tavio*, and H. Alrasyid

Department of Civil Engineering, Institut Teknologi Sepuluh Nopember, Surabaya, Indonesia.

ABSTRACT: Decreased performance of structural members can be caused by several factors, including design errors, modification of building functions, and natural disasters such as earthquakes. In such cases, repairing or strengthening techniques are required to ensure the safety of the structure. Thus, this study experimentally investigated the tensile properties of stainless steel mesh (SSM) as a cost-effective material for strengthening purposes. A total of twelve SSM composite specimens of stainless low density (SLD) and stainless high density (SHD) were tested under tensile loading using a Universal Testing Machine (UTM). The experimental test results show that the SLD2 (stainless low density with two layers) specimen can be used as a promising strengthening material alternative for structural members since it has the highest tensile strength and strain at failure compared to other specimens, i.e. 33.1 N/mm^2 and 33.5%, respectively. However, the SLD1 (stainless low density with one layer) specimen might be an option as an economical/cost-effective strengthening material since its material properties are almost similar to SLD2 by applying only one layer of SSM. All composite specimens exhibited the cup-cone failure mode, indicating that SSM has superior ductility performance. The Tyfo® S epoxy resin provided good adhesion to the SSM.

KEYWORDS: Composite specimens, Economic strengthening, Material properties, Resource efficiency, Stainless steel mesh (SSM).

[Received Oct. 1, 2024; Revised Feb 7, 2025; Accepted Feb 16, 2025] Print ISSN: 0189-9546 | Online ISSN: 2437-2110

I.INTRODUCTION

To obtain optimal performance from a building, its structural members must be carefully designed based on applicable regulations, including proper implementation in the construction process (Agustiar et al., 2018; Anggraini et al., 2018, 2021; Wahjudi, 2014). There are many possible causes for the declining performance of structural members, e.g., design errors in construction, changes in building functions, and natural disasters such as earthquakes are among the causes. Therefore, repairing or strengthening techniques are required to increase the load capacity of structural members such as beams, columns, and beam-column joints (Askar et al., 2022; Pinto et al., 2019). The load capacity of a structural member is the internal capability of a structural member to support or withstand the magnitude of the applied load, such as dead load, live load, and wind load or earthquake load (Zhou et al., 2021). The applied load can cause deformation, stress, and displacement that have the potential to damage the building structures. Beams, columns, and beam-column joints are the main structural members important for maintaining the stability of the building structure (Agustiar et al., 2018). These three structural members make a continuous load path to transmit the loads acting on the building structure to the foundation, and thus the soil. In its application, the reinforcement technique is carried out by attaching reinforcement material to the surface of the structural members. Epoxy resin is used to glue the attached material so it does not come off. Thus, a composite material is obtained that can adhere well to the concrete surface. Therefore, epoxy resin plays an important role in reinforcement techniques (Honestyo et al., 2023).

Many materials are often used to reinforce or strengthen structural members, such as steel plates and non-metallic materials (Machmoed et al., 2020; Sabariman et al., 2020; Tavio et al., 2021; Rafani et al., 2021; Machmoed et al., 2021; Tavio et al., 2022). Steel plates are one of the first materials used for reinforcement, especially in reinforced concrete beams (hereinafter referred to as RC beams). However, there are several disadvantages to the use of steel plates, such as corrosion, weight, and high interfacial tension problems (Zhang et al., 2021). When the steel plate is corroded, it can reduce the effectiveness of its bond with the concrete. In addition, high interfacial tension can cause the concrete to fail early in its compression section. Therefore, steel plate materials cannot provide their benefits optimally (Zhang et al., 2021). Non-metallic materials such as glass, carbon, aramid, and basalt fiber reinforced polymer (GFRP, CFRP, AFRP, and BFRP) are used to resolve the problems associated with steel plates. This is due to their high strength-to-weight ratio, corrosion resistance, and easy applicability (Sohail et al., 2021). Nevertheless, this material still has a very high price. Thus, limiting its widespread application, especially in low-rise buildings and houses or residences (Naser et al., 2019). Therefore, currently, there is a more economical reinforcement

*Corresponding author: tavio@its.ac.id

doi: http://dx.doi.org/10.4314/njtd.v22i1.2944

material innovation, namely Steel Reinforced Polymer (SRP). SRP is a composite material that combines the high strength of steel with a polymer matrix (epoxy resin). In recent years, SRP materials have attracted the attention of many researchers, due to their high tensile strength and corrosion resistance (Hao et al., 2022). SRP materials that have high tensile strength and corrosion resistance can help structural elements withstand large tensile loads, as well as make them have a long life. In addition, it is easily available at a quite low price. Types of SRP materials available in the local market especially in Indonesia, such as galvanized steel mesh (GSM), stainless steel mesh (SSM), and steel wire mesh (SWM).

In recent years, many studies have been conducted to investigate the effectiveness of SRP as a strengthening material for structural members. The use of GSM material as strengthening of RC beams with the treatment of extreme environmental conditions has been studied (Hawileh et al., 2018; Al Nuaimi et al., 2020; Sohail et al., 2021; Hao et al., 2022; Hawileh et al., 2022), and the result is that GSM can increase the ultimate load capacity, stiffness, energy absorption, and ductility of RC beams. Meanwhile, delamination failure mode occurs, indicating that GSM has a good bond with concrete compared to CFRP, which causes debonding failure. SWM as flexural strengthening of beams has been studied by Qeshta et al. (2015). The results of hybrid SWM with CFRP showed better load-deflection curves and were able to prevent debonding failures in CFRP so that CFRP fully provided its benefits. However, SWM embedded in cement mortar, also known as ferrocement, has proven to be an effective and economical material for RC beam strengthening. Ferrocement as torsion strengthening in RC beams has been conducted (Behera et al., 2016; Rajguru and Patkar., 2022; Alzabidi et al., 2023). The results proved that ferrocement can increase the torsion capacity of RC beams. In addition, significant results occurred in the U-wrapping ferrocement strengthening configuration. On the other hand, using ferrocement as a shear-strengthening material, it was found that increasing the number of expanded and welded mesh layers can increase the ultimate load, load deflection, stiffness, toughness, and shear stress of ferrocement-strengthened beams (El-Sayed and Erfan, 2018).

Stainless steel mesh (SSM) is a versatile material made from a combination of stainless steel wires welded or woven to form a grid or net. SSM is widely used in industrial, commercial, and household applications due to its strength, durability, and resistance to corrosion. SSM was utilized as torsion strengthening in RC beams (Patel et al., 2018). The torsional capacity of the RC beam is better increased when corner and diagonal strip coating configurations are used. To increase the compressive capacity of circular concrete columns, SSM material was developed by Kumar and Patel, (2016). The results showed that the axial compressive strength of the columns increased by 61% and 86%, respectively, when SSM with one and two layers was applied. Therefore, compared to CFRP and GFRP, SSM can be used as a cost-effective strengthening for concrete columns.

However, to increase the confidence of researchers, experimental results are usually compared with theoretical analysis. The main purpose of theoretical analysis is to evaluate and ensure that experimental results are safe when applied to existing conditions. To obtain accurate theoretical analysis values, it is necessary to know the material properties of a material used by conducting tests. Therefore, tensile testing is one of the tests carried out to identify the tensile strength of a material. This test is carried out by pulling the material specimen until it breaks so that the test results obtain data such as modulus of elasticity (E), yield strength (f_y), ultimate strength (f_u), and strain at failure (ε). By understanding the properties of materials, researchers can make informed decisions that ensure safety, efficiency, and innovation. Tensile and bonding tests of SSM have been conducted by Patel et al. (2023, 2024). Using three different variations of Indian product SSM, it was found that SSM has a tensile strength range of around 489-658 MPa which is comparable to the tensile strength of different types of fibers used for strengthening. The 40×32 SSM is better in terms of tensile strength and bond strength. Hence, it can be used as an alternative innovation for RC beam strengthening as compared to FRP material and the cup-cone failure mode that occurred in each of the SSM specimens. Welded wire mesh and hexagonal metal mesh were subjected to tensile tests by Tanawade and Modhera (2017). Welded wire mesh was subjected to tensile tests with different orientations 0˚, 30˚, and 45˚. As a result, Ø2.7-mm welded mesh with orientation 0˚ is better than Ø2.3-mm mesh, and the ductility of hexagonal metal mesh has good behavior. Ferrocement with SSM was carried out using tensile test by Fang (2020). Ferrocement samples with variations in the number of SSM layers of one, two, and four were made. The results indicate that the increase in yield and peak load can be up to two or four times, according to the number of SSM layers used. Once the first transverse crack appeared, all of the specimens in the failure mode of mortar cracked suddenly.

However, at present, the evaluation of the tensile strength of composite SSM specimens with epoxy is still limited. Therefore, this study aims to investigate the tensile strength of composite SSM, especially the Indonesian products, and compare it with ferrocement SSM that has been studied by Fang (2020).

II. MATERIALS AND METHODS

A. Materials

1). Stainless steel mesh

Stainless Steel Mesh (SSM) is a wire mesh made of stainless steel wire. SSM is commonly used in various industries because of its durability, strength, and resistance to corrosion. Stainless steel is chosen to be used as a material for various products because this stainless steel material has several special characteristics or natural properties, including acid resistance, alkali resistance, heat resistance, and wear resistance. With the many benefits offered, stainless steel has an important role in the world of infrastructure, especially as a strengthening material. Stainless steel wire mesh comes in two types: Dutch Weave and Square Opening. Meanwhile, the square opening can be divided into two, namely: plain and twill weaves (PT. SIKMA, 2022). The plain weave is the most

widely used type of weave. Each wrap wire alternately passes through the top and bottom of the weft wire at right angles, and vice versa. The opening is square, and the wire uses the same diameter as the wrap and weft wires. The twill weave is similar to plain weave, except that the weft wires alternately pass over and under two wrap wires instead of just one, in a zigzag manner. Both types of stainless steel mesh are shown in Figure 1.

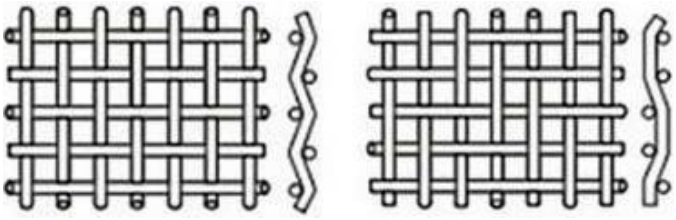

(a) Plain weave (b) Twill weave

Figure 1 a). Wire mesh - plain weave b). Wire mesh - twilled weave

In this study, plain weave stainless steel mesh with the following specifications was used, namely stainless low density (SLD) with a mesh width of 3.73 mm, wire diameter of 0.5 mm, and stainless high density (SHD) with a mesh width of 0.37 mm, wire diameter of 0.14 mm. Both products are already available in the local market, especially in Indonesia.

2). Epoxy

Although there are several adhesives on the market, epoxy resin is one of the most commonly used to strengthen structural elements. This adhesive is a type of synthetic adhesive made from organic adhesives and is classified as a type of thermosetting resin. The two-component epoxy resin consists of components A and B, which can harden when mixed with the appropriate ratio according to the manufacturer. In this study, this type of adhesive was used to make SSM composite materials is Tyfo® S Saturant Epoxy by PT. FYFE Fibrwrap Indonesia (2022).

B. Composite SSM Specimens

At the first stage, the composite SSM specimen preparation commenced by making a special rectangular glass mould. The rectangular mould has dimensions of 19 mm width and 165 mm length, as shown in Figure 2.

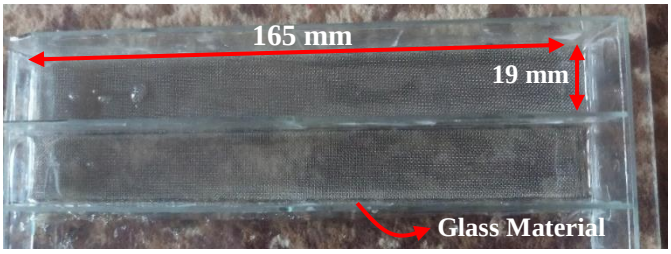

Figure 2 Rectangular mold of composite SSM specimens

The second stage involved mixing the epoxy according to the manufacturer's instructions (PT. FYFE Fibrwrap Indonesia, 2022) to obtain good composite materials. Epoxy consists of two parts, namely part A and part B. The two parts are mixed in a ratio based on volume (A: B = 100 ml: 0.42 ml). First, part A is poured into part B, then mixed by stirring for 5 minutes or until evenly mixed. After that, place the SSM that has been cut according to the dimensions of the mold, followed by pouring the evenly mixed epoxy into the mold to the height of the composite SSM specimen. Then, the composite SSM specimen is left for three days for the curing process.

In the third stage, the SSM that has become a composite is formed into a coupon test using a Maktek MT90-type grinding machine according to ASTM E8/E8M−24 (2024). The SSM composite specimen has been formed into a coupon test, as shown in Figure 3.

Figure 3 The composite SSM specimens

Twelve SSM composite specimens were subjected to tensile testing, namely the SLD-1 specimen and SLD-2 specimen with three specimens each, then the SHD-1 specimen and SHD-2 specimen with three specimens each (see Figure 3). Detailed dimensions of each composite SSM specimen are shown in Figure 4. The symbols on each specimen are SLD1-1 for SSM low density one layer; SLD2-1 for SSM low density two layers; SHD1-1 for SSM high density one layer; and SHD2-1 for SSM high Density two layers.

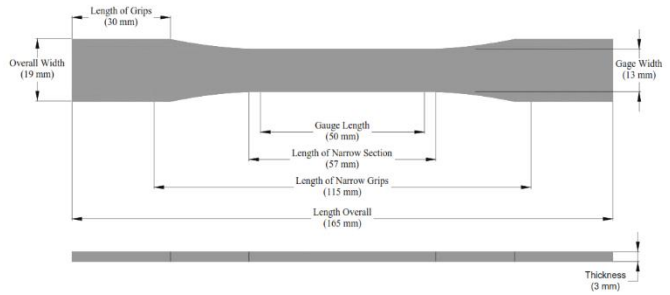

Figure 4 Detailed dimensions of the composite SSM specimens

C. The Tensile Test Setup of SSM Specimens

To determine the mechanical properties of a material, testing is required. One of the most frequently performed tests is the tensile test. The tensile test provides information on the strength and ductility of the material under uniaxial tensile stress. In this study, the tests were conducted using a Hung TA

HT-2402 UTM machine, which had a load capacity of 1 kN, as shown in Figure 5. The tensile load application rate was based on ASTM D3039/D3039M–17 (2017). The composite SSM specimen was subjected to tensile testing until the specimen failed, which was indicated by fracture. During the test, the elongation, yield strength, and ultimate strength data of the SSM specimen were automatically recorded by the machine and then transferred to the computer, where the final result was a stress-strain curve. The test was conducted based on ASTM E8/E8M–24 (2024).

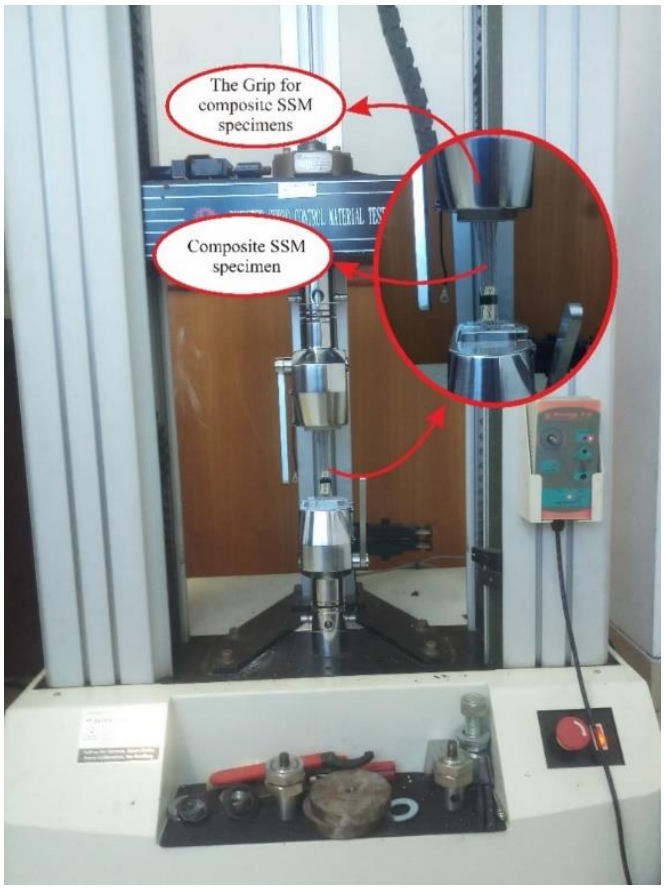

Figure 5 The tensile test of SSM specimens on a UTM machine

a) RESULTS AND DISCUSSION

A. The Failure Mode of SSM Composite Specimens

Figure 6 shows the failure mode of all composite SSM specimens. The stainless low-density (SLD) specimen experienced a different failure mode from the stainless high-density (SHD) specimen, where the epoxy resin in the SLD specimen had several cracks, while in the SHD specimen, only one crack occurred. The cracking of the epoxy resin was due to the relatively lower tensile strength of the epoxy resin, compared to SSM, which has a higher tensile strength. One of the factors that affects the tensile strength of the epoxy resin is the mixture composition between components A and B, where, in this study, the mixture design followed the manufacturer's guidelines.

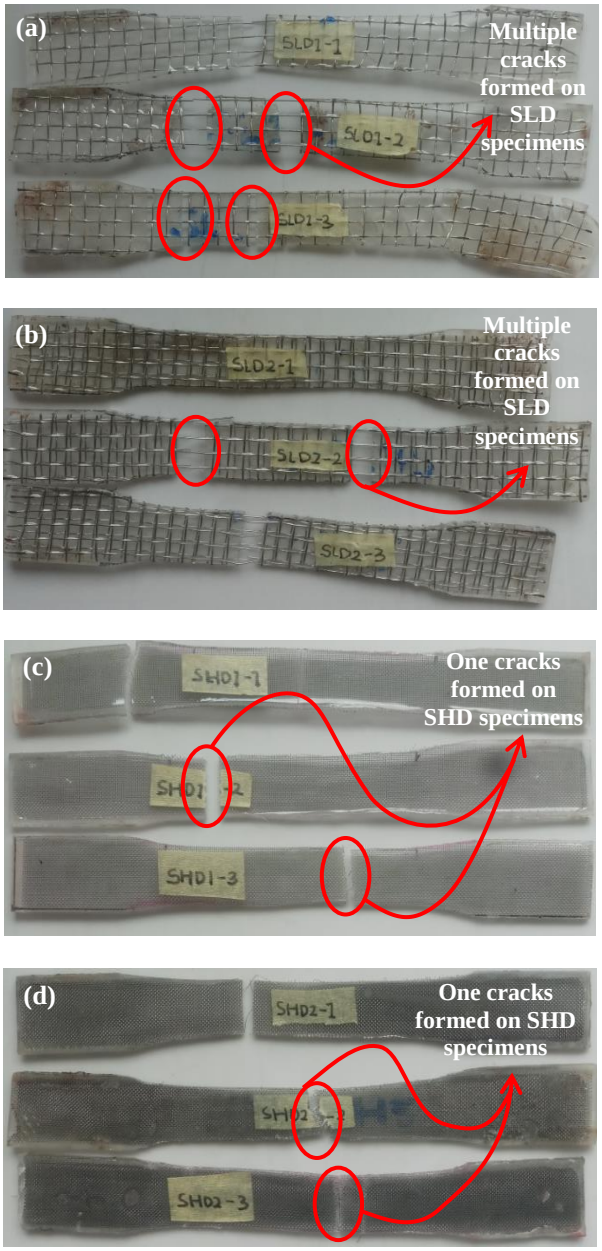

Figure 6 Failure mode of SSM composite specimens after tensile testing, a) SLD1, b) SLD2, c) SHD1, and d) SHD2

The occurrence of several cracks in the SLD1 and SLD2 specimens was caused by the higher tensile strength of SLD compared to epoxy resin. When the initial load was given, SLD and epoxy resin still showed elastic conditions, so that no cracks were seen. When the load continued to increase, the epoxy resin cracked. At this time, the epoxy resin had reached its tensile strain capacity, while the SLD material still showed its capability to withstand the given tensile load. When the load continued to increase, approaching its ultimate, several cracks occurred in the epoxy resin until the SLD finally failed. In addition, the SLD material had a larger wire diameter than the SHD material. Thus, it was possible to have a greater tensile capacity. Therefore, several cracks formed in the SLD1 and SLD2 specimens during the tests.

Meanwhile, SHD1 and SHD2 specimens experienced the same failure mode, which was the formation of one crack.

However, in the SHD1 specimen, when the crack occurred, the SSM suddenly broke completely, while the SHD2 specimen did not fracture completely. Figures 6c and 6d show the failure modes of specimens SHD1 and SHD2, respectively. When the SHD1 specimen approached its ultimate load, the tensile stress that occurred was completely concentrated on that one layer. As a result, the SSM material reached the plastic deformation limit faster because it had to withstand all the tensile stress that occurred. This could cause failure of the SSM with one layer to break completely. While in the SHD2 specimen, the tensile stress was evenly distributed between the two layers. Thus, it allowed the layers to work together to withstand deformation. As a result, the SSM with two layers did not break completely. When the SHD1 specimen broke, it could be seen that the SSM and epoxy resin also broke simultaneously. This indicated that the tensile strength of the SSM and epoxy resin were almost the same, 12.5 N/mm^2, as shown in Table 1. It should be noted that this only occurred in high-density specimens with one layer. While the SHD2 specimen during the test showed that the SSM and epoxy resin did not break simultaneously, because the SSM with two layers was able to slow down the crack widening that occurred in the epoxy resin. When the crack began to develop, the energy from the crack was evenly distributed between the two layers of SSM. This caused the energy available to extend or widen the crack in the epoxy resin to be reduced, thus slowing down the process.

Figure 7 shows the stress-strain curve of SSM composite specimens, indicating the stainless low density 1 layer in (a), stainless low density 2 layer in (b), stainless high density 1 layer in (c), and stainless high density 2 layer in (d). The stress-strain curves of the SLD and SHD specimens also show differences, as shown in Figures 7a and 7b, where the SLD specimen curve goes up and down. This phenomenon is similar to the experimental tests conducted by (Patel et al., 2023, 2024). This is due to the occurrence of cracks in the epoxy resin when the tensile load is applied. Meanwhile, the curves on the SHD specimens are slightly smoother, as shown in Figures 7c and 7d. This difference indicates that stainless wire with a large diameter, such as the SLD specimen, can slow down crack widening in epoxy resin better.

It should be noted that the SLD2-1 specimen failed during the tensile test, so this specimen showed an imperfect curve and could not be used, as shown in Figure 7b. This is due to the grip on the UTM machine that could not grip the specimen properly. As a result, the SLD2-1 specimen was released from the UTM grip.

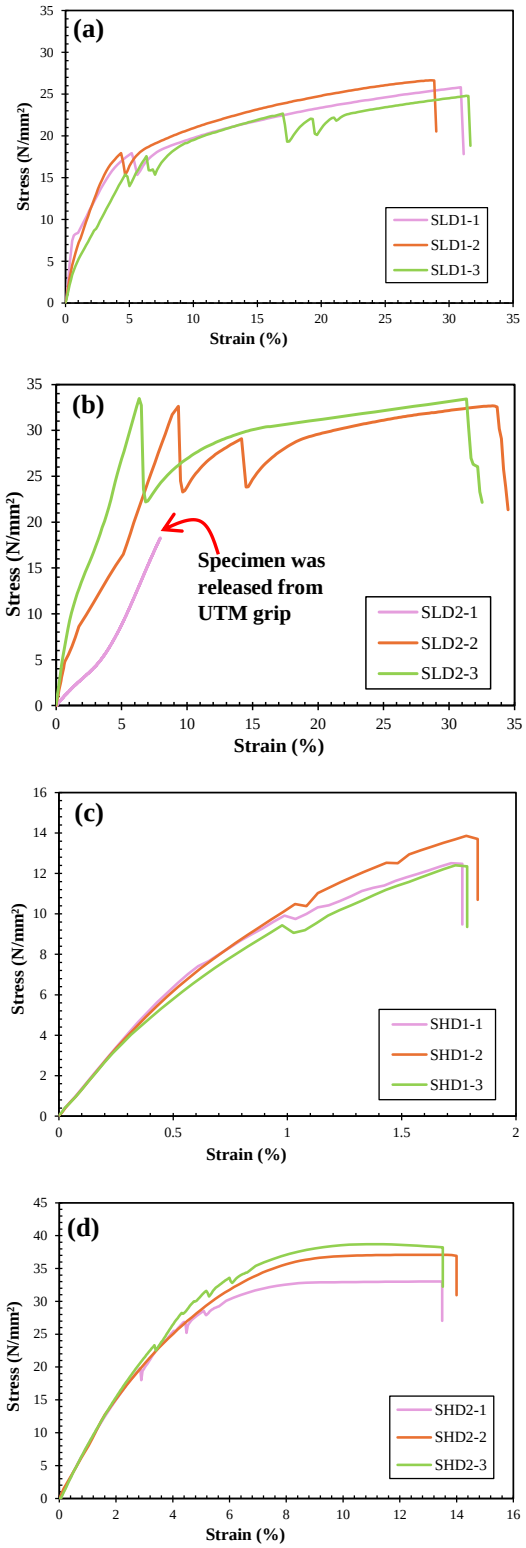

Figure 7 Stress-strain curve of SSM composite specimens, a) Stainless Low Density 1 layer, b) Stainless Low Density 2 layer, c) Stainless High Density 1 layer, d) Stainless High Density 2 layer

Table 1 Average result of tensile test SSM composite specimens

Material	Elastic modulus (N/mm^2)	Yield strength (N/mm^2)	% Increase	Tensile strength (N/mm^2)	% Increase	Strain at rupture (%)	% Increase
SLD-1	475	18.3	-	25.7	-	30.3	-
SLD-2	382	26.9	32	33.1	22	33.5	9.5
SHD-1	1180	7.0	-	12.5	-	1.8	-
SHD-2	778	27.2	74	37.9	67	13.8	87

The fracture of the wire mesh on each specimen occurred as the load approached its ultimate. Based on the research of (Patel et al., 2023, 2024), the fracture of the wire mesh typically forms a failure mode commonly called a cup-cone, as shown in Figure 8. The cup-cone failure mode is the wire end that forms like a cup with a tapered end. In this study, SLD specimens and SHD specimens experienced cup-cone failure mode. Meanwhile, during the tensile test, the composite SSM specimens showed that the stainless steel mesh did not peel off from the composite epoxy resin. This indicates that Tyfo® S Saturant Epoxy has an excellent bond for use in SSM materials.

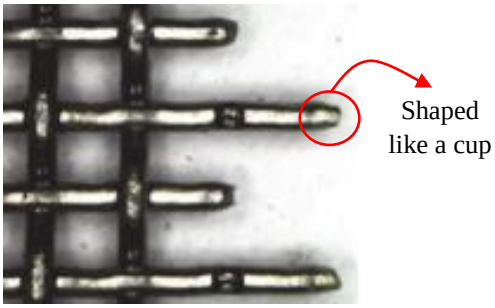

Figure 8 Cup-cone failure mode (Patel et al., 2024, 2023)

B. Material Properties Results of SSM Composite Specimens

Table 1 illustrates that the high-density stainless steel specimen with one layer (SHD1) exhibits the lowest yield strength, tensile strength, and strain values compared to the other specimens, which are about 7 N/mm^2, 12.5 N/mm^2, and 1.8%, respectively. When the SHD1 specimen is subjected to tensile loading, the stress-strain curve increases. However, when the load reaches its ultimate, the stress-strain curve decreases suddenly, which is indicated by the fracture of the stainless steel wire, as shown in Figure 6c. The stainless steel mesh on the SHD1 specimen makes almost no contribution to resisting the tensile load. Meanwhile, the SHD2 specimen with two layers has higher yield strength, tensile strength, and strain at failure values than the SHD1 specimen, which are 27.2 N/mm^2, 37.9 N/mm^2, and 13.8%, as shown in Table 1. This is because the SSM was installed in two layers on the SHD2 specimen. The SSM on the SHD2 specimen can resist the tensile load better than the SHD1 specimen so the SSM experiences a higher elongation. From Table 1, it is known that SHD2 experienced an increase with each percentage of 74%, 67%, and 87% compared to the SHD1 specimen.

Different results were obtained from the stainless low-density (SLD) specimen. The SLD2 specimen showed higher yield strength, tensile strength, and strain values compared to the SLD1 specimen, which were 26.9 N/mm^2, 33.1 N/mm^2, and 33.5%, respectively. Table 1 shows that the percentage increase in the SLD2 specimen was 32%, 22%, and 9.5% in the SLD1 specimen. This increase is due to the SSM with two layers being able to withstand the tensile load given well. In addition, factors that affect the increase in material properties of the SLD2 specimen are the diameter and distance of the wire, which are 0.5 mm and 3.73 mm, respectively. The larger distance between the wires allows the epoxy resin to fill the gaps perfectly. Then, the tensile stress that occurs in the SLD2 specimen can be evenly distributed between the two layer areas. Thus, this allows the SLD2 specimen to work in withstanding the tensile load given with a greater capacity.

When the tensile load was applied and continued to increase, the SLD2 specimen was still able to provide resistance even though cracks had formed. However, as the load approached its ultimate value, some of the wires in the SLD2 specimen ruptured but did not rupture completely. Thereafter, the stress-strain curve decreased quite significantly, as shown in Figures 7a and 7b. The percentage increase from SLD2 to SLD1 is small. This means that the material properties of specimens SLD2 and SLD1 are almost similar, as shown in Table 1.

If the SLD specimen is compared with the SHD specimen, the SHD2 specimen has a higher tensile strength than the SLD2 specimen, which is 37.9 N/mm^2 and 33.1 N/mm^2, respectively. The difference is very small, around 13%. However, SHD2 has a much smaller strain capacity than the SLD2 specimen, which is 13.8% and 33.5%, respectively. The difference is more than half, which is around 59%. Therefore, the SHD specimen cannot be selected as a strengthening material, because the strain capacity is one of the mechanical properties that need to be considered. The greater the strain capacity value, the greater the structure's ability to withstand. When the structural member with the strengthening material approaches its ultimate capacity, the strengthening material will provide resistance to the forces that occur. Therefore, crack formation can be slowed down with strengthening materials (Hawileh et al., 2022). The SLD2 specimen is a recommended material for use as a reinforcement for structural elements, such as RC beams and circular columns. This specimen has a higher yield strength, tensile strength, and strain compared to other specimens. From Table 1, the values are 26.9 N/mm^2, 33.1 N/mm^2, and 33.5%, respectively. In addition, the SLD1 specimen has almost the same yield strength, tensile strength, and strain values as the SLD2 specimen. From Table 1, it is known that each has a percentage difference of 32%, 22%, and

9.5%. Therefore, this specimen can be selected as an economical reinforcement material, because this specimen only has one layer of SSM.

C. Modulus of Elasticity of Composite SSM Specimens

The elastic modulus of the SSM composite specimen is affected by the number of SSM layers installed. From Table 1, it can be seen that the elastic modulus value of the SLD1 specimen is greater than that of SLD2, which is 475 N/mm^2 and 382 N/mm^2, respectively. It is known that the SLD1 specimen only has 1 SSM layer while the SLD2 specimen has two SSM layers. The same phenomenon occurs in the SHD specimen. The elastic modulus of the SHD1 and SHD2 specimens from Table 1 are 1180 N/mm^2 and 778 N/mm^2, respectively. It can be observed that there is a negative correlation between the elastic modulus and the strain capacity. In other words, the greater the elastic modulus, the smaller the strain capacity. In addition, the elastic modulus is influenced by the ratio of epoxy resin composition. In this study, compositions were made in accordance with the instructions provided by the manufacturer. Therefore, further research is required to obtain an effective composite SSM material, with variations in the ratio between the different A: B components.

D. Failure Mode Comparison between Epoxy Composite SSM and Ferrocement SSM

The failure mode of the epoxy composite SSM specimen and the ferrocement SSM specimen is similar, namely, the formation of multiple cracks, as shown in Figure 9.

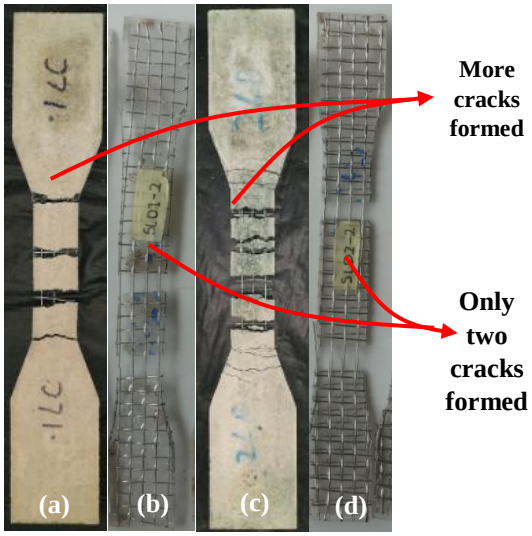

Figure 9 Comparison of ferrocement SSM and epoxy composite SSM, a) and b) SSM with 1 layer, c) and d) SSM with 2 layers

It is known that the ferrocement SSM formed multiple cracks with increasing load (Fang, 2020). This is caused by the lower tensile strength of the cement material compared to the epoxy SSM composite material. Figures 9a and 9c are ferrocement SSM tensile tested by (Fang, 2020). The SSM specifications used are SSM with a mesh width and wire diameter of 8.5 mm and 1.0 mm, respectively. The variations in the number of SSM layers used are one layer and two layers, respectively. It can be observed that both specimens formed several cracks after the tensile test. However, the epoxy composite SSM specimen has fewer cracks than the ferrocement SSM specimen. This means that the epoxy resin has better tensile strength than the cement material.

E. Determination of yield stress of composite SSM specimens

Yield stress (or yield strength) is defined as the amount of stress at which a material begins to deform plastically. Before reaching the yield point, a material will deform elastically, exhibiting the capacity to return to its original shape once the stress is removed. However, when the yield stress is exceeded, the material will undergo permanent deformation, losing its ability to return to its original shape (Anggraini et al., 2018). The yield stress (P_y) of the composite SSM specimen is determined by identifying the point of intersection between the best straight line of the initial section of the stress-strain curve and the best straight line of the yield section of the stress-strain curve (ACI PRC-549.1-18, 2018).

Figures 9a and 10b illustrate the stages of stress-strain curve formation for SHD and SLD specimens. The formation of the stress-strain curve for SHD specimens can be divided into four stages, as shown in Figure 9a. In Stage I, the SHD specimen is still in an elastic condition, where the stress-strain curve remains linear. In Stage II, the stress-strain curve is slightly curved. At this stage, the SHD specimen is in a transitional state from elastic to yielding (inelastic). The yield stress is determined by drawing a straight line at the initial stress until it intersects with a straight line at the point where the stress-strain curve is in the transitional state from yielding to a state of hardening. Then, draw a straight line from the intersection point to the stress-strain curve. In Stage III, the stress-strain curve exhibits an increase in height until it finally reaches its ultimate stress. At this stage, the SHD specimen is in a transitional state from yielding to hardening. In Stage IV, the stress-strain curve shows a decrease until it finally drops more drastically, indicating that the SHD specimen has reached its failure point. At this stage, the SHD specimen is in a state of necking and fracture.

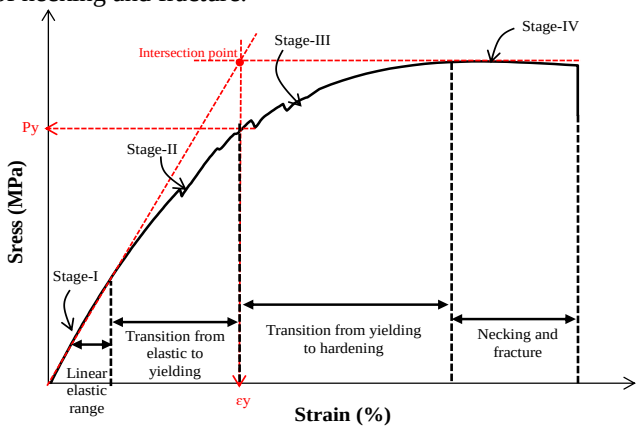

Figure 10 Stages of SHD specimen stress-strain curve formation

The formation of the stress-strain curve of the SLD specimen can be divided into five stages, as shown in Figure 10b. In Stage I, the stress-strain curve is still linear, indicating that the SLD specimen is still in an elastic condition. In Stage II, the stress-strain curve decreases suddenly, which is caused by the cracking of the epoxy resin. In Stage III, the stress-strain curve becomes curved, which indicates the yielding of the SSM. At this stage, the SLD specimen is undergoing a transition from elastic to yielding (inelastic). The yield stress can be identified by taking the midpoint between the two lines at the top and bottom of the stress-strain curve. In Stage IV, the stress-strain curve decreases suddenly, a condition that is similar to that observed in Stage II. In Stage V, the stress-strain curve increases significantly until it reaches the ultimate stress. At this stage, the SLD specimen is in a state of transition between yielding and hardening. In Stage VI, the stress-strain curve decreases significantly and shows no increase in strength, due to fracture of the SLD specimen. At this stage, the SLD specimen is in the necking and fracture state.

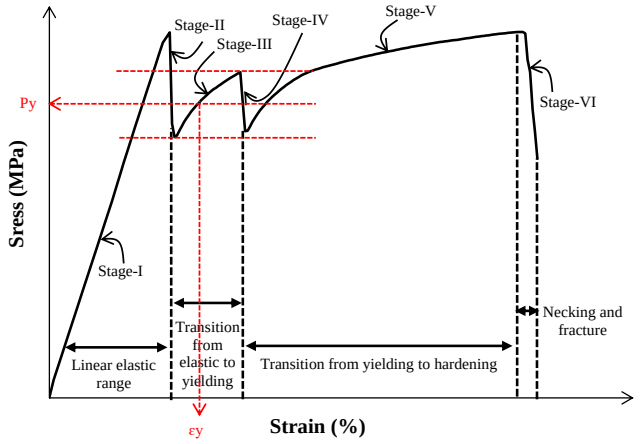

Figure 11 Stages of SLD specimen stress-strain curve formation

IV. CONCLUSION

The main objective of this study was to evaluate the mechanical properties of stainless steel mesh (SSM) composites, including modulus of elasticity, tensile strength, yield strength, and strain at failure. A total of twelve SSM composite specimens with High Density (SLD) and Low Density (SHD) variations were considered for this investigation. Based on the experimental test results, it was concluded that all SSM composite specimens experienced the same failure mode, namely cup-cone. The cup-cone failure mode demonstrated superior ductility performance of the stainless steel mesh composites. Then the stainless steel mesh did not appear to peel off from the composite epoxy resin during the test, indicating that Tyfo® S Saturant Epoxy had good bonding with the SSM material. The performance of the SLD2 specimen was superior to other SSM composite specimens in terms of tensile strength and strain at failure. The tensile strength of the SLD2 specimen was 33.1 N/mm^2, while the strain at failure was 33.5%. It can be recommended that SLD2 specimens be used as innovative reinforcement materials for structural components such as RC beams and circular columns. In addition, the SLD1 specimen can be an option as an economical reinforcement material, because it has a percentage difference in tensile strength and strain at failure that is too far from the SLD2 specimen, namely 22% and 9.5%. The use of reinforcement material with SSM ferrocement has the potential for more cracks than SSM epoxy composite. This means that epoxy resin has better tensile strength than cement material.

AUTHOR CONTRIBUTIONS

Harsono: Methodology, Software, Validation, Writing – original draft & editing**. Tavio:** Conceptualization, Supervision, Writing – original draft, review & editing**. H. Alrasyid:** Writing – review & editing**.**

ACKNOWLEDGEMENT(S)

The authors gratefully acknowledge financial support from the Institut Teknologi Sepuluh Nopember for this work, under the project scheme of the Publication Writing and IPR Incentive Program (PPHKI) 2025.

REFERENCES

ACI PRC-549.1-18. (2018). Design guide for ferrocement. *American Concrete Institute*.

Agustiar; Raka, I. G. P. and Anggraini, R. (2018). Behavior of concrete columns reinforced and confined by high-strength steel bars. *International Journal of Civil Engineering and Technology*, *9*(7), 1249–1257.

Al Nuaimi, N.; Sohail, M. G.; Hawileh, R. A.; Abdalla, J. A. and Douier, K. (2020). Durability of reinforced concrete beams strengthened by galvanized steel mesh-epoxy systems under harsh environmental conditions. *Composite Structures*, *249*, 112547.

Alzabidi, S. M.; Diaa, G.; Abadel, A. A.; Sennah, K. and Abdalla, H. (2023). Rehabilitation of reinforced concrete beams subjected to torsional load using ferrocement. *Case Studies in Construction Materials*, *19*, e02433.

Anggraini, R.; Raka, I. G. P. and Agustiar. (2021). Flexural capacity of concrete beams reinforced with high-strength steel bars under monotonic loading. *International Journal of GEOMATE*, *20*(77), 173–180.

Anggraini, R.; Raka, I. G. P. and Agustiar. (2018). Stress-strain relationship of high-strength steel (HSS) reinforcing bars. *AIP Conference Proceeding*, *1964*, 020025.

Askar, M. K.; Hassan, A. F. and Al-Kamaki, Y. S. S. (2022). Flexural and shear strengthening of reinforced concrete beams using FRP composites: A state of the art. *Case Studies in Construction Materials*, *17*, e01189.

ASTM D3039/D3039M−17. (2017). Standard test method for tensile properties of polymer matrix composite materials. *American Standard Testing and Materials*.

ASTM E8/E8M−24. (2024). Standard test methods for tension testing of metallic material. *American Standard Testing and Materials*.

Behera, G. C.; Rao, T. D. G. and Rao, C. B. K. (2016). Torsional behavior of reinforced concrete beams with ferrocement U-jacketing–Experimental study. *Case Studies in Construction Materials*, *4*, 15–31.

El-Sayed, T. A. and Erfan, A. M. (2018). Improving shear strength of beams using ferrocement composite. *Construction and Building Materials*, *172*, 608–617.

Fang, S. (2020). Axial compressive performance of corroded concrete columns strengthened by alkali-activated slag ferrocement jackets. *Frontiers in Materials*, *7*, 567777.

Hao, R.; Lin, W.; Al-Nuaimi, N. A.; Hawileh, R. A.; Abdalla, J. A. and Elshafie, M. Z. E. B. (2022). Short-term and long-term behavior of RC beams strengthened by galvanized steel mesh laminate. *Construction and Building Materials*, *340*, 127763.

Hawileh, R. A.; Al Nuaimi, N.; Nawaz, W.; Abdalla, J. A. and Sohail, M. G. (2022). Flexural and bond behavior of concrete beams strengthened with CFRP and galvanized steel mesh laminates. *Practice Periodical on Structural Design and Construction*, *27*, 04021068.

Hawileh, R. A.; Nawaz, W. and Abdalla, J. A. (2018). Flexural behavior of reinforced concrete beams externally strengthened with hardwire steel-fiber sheets. *Construction and Building Materials*, *172*, 562–573.

Honestyo, A. and Ardhyananta, H. (2023). Axial compressive behavior of bubble-size plastic straw waste FRP-confined circular concrete. *International Journal on Engineering Applications*, *11*(2), 73–80.

Kumar, V. and Patel, P. V. (2016). Strengthening of axially loaded circular concrete columns using stainless steel wire mesh (SSWM)–Experimental investigations. *Construction and Building Materials*, *124*, 186–198.

Machmoed, S. P. and Raka, I. G. P. (2021). Performance of square reinforced concrete columns confined with innovative confining system under axial compression. *International Journal of GEOMATE*, *21*(85), 137–144.

Machmoed, S. P. and Raka, I. G. P. (2020). Potential of new innovative confinement for square reinforced concrete columns. *IOP Journal of Physics: Conference Series*, *1469*, 012027.

Naser, M. Z.; Hawileh, R. A. and Abdalla, J. A. (2019). Fiber-reinforced polymer composites in strengthening reinforced concrete structures: A critical review. *Engineering Structures*, *198*, 109542.

Patel, P. V.; Joshi, D. D. and Makawana, R. V. (2024). Investigating mechanical properties of stainless-steel wire mesh through experimental studies. *Science Talks*, *9*, 100294.

Patel, P. V.; Joshi, D. D. and Makawana, R. V. (2023). Experimental studies to evaluate the tensile and bond strength of Stainless-Steel Wire Mesh (SSWM). *Frattura ed Integrita Strutturale*, *17*(65), 257–269.

Patel, P. V.; Raiyani, S. D. and Shah, P. J. (2018). Torsional strengthening of RC beams using stainless steel wire mesh–Experimental and numerical study. *Structural Engineering and Mechanics*, *67*(4), 391–401.

Pinto, D. and Raka, I. G. P. (2019). Axial compressive behavior of square concrete columns retrofitted with GFRP straps. *International Journal of Civil Engineering and Technology*, *10*(1), 2388–2400.

PT. FYFE Fibrwrap Indonesia. (2022). Tyfo ® S Epoxy, Indonesia. *Available online at: http://www.fyfeco.com*.

PT. SIKMA. (2022). Stainless steel wire mesh. *Available online at: http://www.ptsikma.com/product-details/stainless-steel-wire-mesh/*.

Qeshta, I. M. I.; Shafigh, P. and Jumaat, M. Z. (2015). Flexural behavior of RC beams strengthened with wire mesh-epoxy composite. *Construction and Building Materials*, *79*, 104–114.

Rafani, M.; Soehardjono, A.; Wisnumurti and Wibowo, A. (2021). A theoretical study of GFRP RC beams deflection, *Journal of Physics: Conference Series*, *1477*, 052047.

Rajguru, R. S. and Patkar, M. (2022). Torsion behavior of strengthened RC beams by ferrocement. *Materials Today Proceedings*, *61*(2), 138–142.

Sabariman, B.; Soehardjono, A.; Wisnumurti and Wibowo, A. (2020). Stress-strain model for confined fiber-reinforced concrete under axial compression. *Archives of Civil Engineering*, *66*(2), 119–133.

Sohail, M. G.; Al Nuaimi, N.; Hawileh, R. A.; Abdalla, J. A. and Douier, K. (2021). Durability of plain concrete prism strengthened with galvanized steel mesh and CFRP laminates under harsh environmental conditions. *Construction and Building Materials*, *286*, 122904.

Tanawade, A. G. and Modhera, C. D. (2017). Tensile behaviour of welded wire mesh and hexagonal metal mesh for ferrocement application. *IOP Conference Series: Material Science Engineering*, *225*, 012069.

Tavio; Machmoed, S. P. and Raka, I. G. P. (2022). Behavior of square RC columns confined with interlocking square spiral under axial compressive loading. *International Journal on Engineering Applications*, *10*(5), 322–335.

Tavio; Rafani, M.; Raka, I. G. P. and Ratnasari, V. (2021). Flexural capacity predictions and comparisons of GFRP reinforced beams. *Journal of Physics: Conference Series*, *1477*, 052049.

Wahjudi, D. I. (2014). Behavior of precast concrete beam-to-column connection with U- and L-bent bar anchorages placed outside the column panel–experimental study. *Procedia Engineering*, *95*(2014), 122–131.

Zhang, J.; Xu, Y.; Mai, Z. and Lv, W. (2021). Flexural performance of RC T-beams strengthened with external double steel channel. *Journal of Building Engineering*, *42*, 102453.

Zhou, Y.; Shao, H.; Cao, Y. and Lui, E. M. (2021). Application of buckling-restrained braces to earthquake-resistant design of buildings: A review. *Engineering Structure*s, 246, 112991.